Nonlinear oscillations of gas bubbles in liquids: An interpretation of some experimental results

Lawrence A. Crum
Physical Acoustics Research Laboratory, Department of Physics, University of Mississippi, Oxford, Mississippi 38677

Andrea Prosperetti
Istituto di Fisica, Universita di Milano, Milan, Italy

(Received 6 July 1982; accepted for publication 29 September 1982)

Measurements are presented in this paper of the pulsation amplitude of an individual air bubble that is levitated in a glycerine–water mixture by a stationary acoustic wave operating at a frequency of 22.2 kHz. Observations of the bubble pulsation for a wide range of bubble sizes demonstrate the existence of the $n = 2$ harmonic resonance ($\omega \approx \omega_0/2$). The available theoretical information on linear and nonlinear bubble oscillations is adapted to apply to the specific experimental conditions. Comparisons made with the theory show excellent agreement between measurements and predictions.

PACS numbers: 43.25.Yw, 43.25.Qb

INTRODUCTION

In recent years there has been considerable theoretical activity concerning the nonlinear aspects of bubble oscillations, by both numerical[1] and approximate analytical techniques.[2–5] This interest has been motivated by the experimentally established connection between subharmonic emissions and the presence of cavitation activity in a variety of experimental conditions.[6–14] Experimental investigations involving nonlinear oscillations of single bubbles has been primarily confined to the subharmonic region, although there have been some recent investigations of the harmonics.[15,16] In this paper we wish to concentrate in the area of the harmonic activity in both a theoretical and experimental manner. We wish to demonstrate the existence of harmonic activity in an individual bubble, to adapt the pertinent theory to our experimental conditions, and to show the predictions of the theory agree remarkably well with the experimental observations.

I. EXPERIMENTAL APPARATUS AND TECHNIQUE

Measurements of the pulsation amplitude of an individual gas bubble were made by acoustically levitating the air bubble near an antinode of an acoustic stationary wave. This technique[17–19] is becoming commonplace as a method for measuring the properties of individual gas bubbles as well as other particles[19] and will not be discussed in detail in this paper. For completeness, however, a short description of the method is given.

A compressible particle that is present in an acoustic stationary wave will experience radiation pressure forces that will tend to move it toward or away from the pressure antinodes of the field, depending on certain acoustic properties of the particle and of the liquid. The particle will normally also experience gravitational and hydrostatic forces that may be in opposition to the radiation pressure forces. Accordingly, equilibrium positions exist in the sound field where the net force acting on the particle vanishes. In this condition, the particle can be said to be levitated at a position of stable equilibrium by the sound field. In the case of a gas bubble in a liquid these stable positions are near the antinodes of the sound field when the sound frequency is below the resonance frequency of the bubble. If the liquid is free from other gas bubbles and inhomogeneities which tend to lead to fluctuations in the sound field amplitude, the bubble can be stably positioned to within a diameter or so for a duration of several minutes.

The theory to be discussed below shows that, in the absence of harmonic resonances in the bubble pulsation, the position of the bubble in the sound field depends only weakly on the radius. Thus even if it undergoes some growth by diffusion, its position does not change appreciably. In the neighborhood of a harmonic resonance, however, displacements from this position are predicted by the theory. By measuring these slight displacements in the bubble's position as a function of radius the theory can be put to a stringent test and considerable information about the nonlinear behavior of the oscillations can be gained. The amplitude of these harmonic components depends on the ratio of the driving frequency of the sound field to the resonance frequency of the bubble. Since the resonance frequency is a function of the bubble radius, for a fixed sound frequency, the amplitude can also be expressed in terms of the ratio of the equilibrium radius to the resonance radius. This latter quantity can be easily varied in our experimental system due to the presence of rectified diffusion.

A typical procedure for obtaining measurements of the pulsation amplitude of a gas bubble as a function of its radius and the acoustic driving amplitude is as follows: A bubble whose size is less than its resonance size is introduced into the stationary wave system. It may be introduced via a hypodermic needle, or by simply increasing the amplitude of the acoustic stationary wave until it "appears" due to gaseous cavitation. The levitation cell is typically constructed from two cylindrical ceramic transducers, and sandwiched with a transparent glass cylinder for viewing the bubble (see Fig. 1, Ref. 18). Our particular configuration is approximately 10 cm in height by 7.5 cm in diameter, the gas bubble being levitated along the axis of the cylinder and beneath the glass cylinder, near the middle of the cell. We surround our levitation cell with a second cylinder, concentric with the first, with viewing ports and maintained at a constant temperature. Fluctuations in temperature of the host liquid contained within the levitation cell can greatly reduce our signal-to-noise ratio. We maintain the host fluid at a temperature that makes it slightly undersaturated in terms of its dissolved gas content. Extraneous and unwanted gas bubbles will then dissolve and we can more easily control the size of the bubble of interest. Gas bubbles that are levitated and driven at low sound amplitudes will slowly dissolve, but by increasing the amplitude of the sound field we make the bubble grow to a desirable size by rectified diffusion. This size may be as large as 80% of its resonance size. We then select a value for the acoustic pressure amplitude that is less than, but near the threshold for rectified diffusion and constantly maintain this value. As the bubble slowly dissolves, we make measurements of its size (by turning off the sound field and measuring its terminal rise velocity[17,18]) and its position in the calibrated sound field. The bubble will maintain approximately a fixed position until it approaches a size that is nearly one-half its resonance size (at the fixed driving frequency), and then will undergo a slight but measurable shift in its position. If we know the size and position of the bubble, the amplitude and spatial variation of the sound field, we can then obtain certain components of its pulsation amplitude by use of the equations to be developed in Sec. II below. We then repeat the procedure at a different pressure amplitude. At relatively large pressure amplitudes, it is often desirable to start the bubble at a small size and permit it to grow slowly by rectified diffusion to larger sizes. We try, as much as possible, to make an entire run with a single bubble. They are notorious scavengers, and a well-behaved, clean one is sometimes hard to find. With some practice, one can learn which bubbles will give a consistent set of data.

II. THEORY

The acoustic radiation pressure force on a bubble (or highly compressible particle) in a stationary sound field is often called the primary Bjerknes force and is given by[20]

$$\mathbf{F}_A(\mathbf{r},t) = -\langle V(t)\nabla P(\mathbf{r},t)\rangle , \tag{1}$$

where angle brackets denote time average, $V(t)$ is the instantaneous volume of the bubble and $P(\mathbf{r},t)$ is the time- and space-varying pressure field which can be closely approximated along the axis of the levitation cell used in this experiment by

$$P(\mathbf{r},t) = P_\infty - P_A(z)\cos \Omega t . \tag{2}$$

Here P_∞ is ambient pressure, Ω is the angular frequency of the sound field, and $P_A(z)$ is the space-dependent amplitude of the stationary wave. The coordinate z is measured vertically along the axis of the cell. For a spherical bubble of equilibrium radius R_0 and instantaneous radius $R(t)$, we find the magnitude of the acoustic force, obtained by inserting Eq. (2) into Eq. (1), to be given by

$$F_A = \tfrac{4}{3}\pi R_0^3 |\nabla P_A| \langle [R(t)/R_0]^3 \cos \Omega t\rangle .$$

When the bubble maintains a fixed position in the cell, this force is balanced by the magnitude of the average buoyancy force, viz.,

$$F_B = \tfrac{4}{3}\pi R_0^3 \rho g \langle [R(t)/R_0]^3\rangle ,$$

where ρ is the liquid density and g is the acceleration of gravity. Equating these two forces gives

$$\frac{\langle (R/R_0)^3 \cos \Omega t\rangle}{\langle (R/R_0)^3\rangle} = \frac{\rho g}{|\nabla P_A|}, \tag{3}$$

where $|\nabla P_A|$ is evaluated at the position of the bubble. The ratio of ρg to $|\nabla P_A|$ is essentially the ratio of the hydrostatic pressure gradient to the acoustic pressure gradient. For brevity, and for lack of previous terminology, we shall refer to this quantity as the *levitation number*,

$$\mathscr{L}_e = \rho g / |\nabla P_A| .$$

A large value of this quantity implies that a small acoustic pressure gradient is sufficient to stabilize the bubble against gravity. This in turn implies that the oscillatory regime is such that the acoustic force is exploited very efficiently and conversely for a small value of $\mathscr{L}_e$. In the present study the quantities on the right-hand side of Eq. (3) are either known or measured experimentally, whereas the ratio on the left-hand side is computed theoretically. Therefore the results to be described below can be viewed as comparisons between the theoretical and experimental values of the levitation number.

The time-varying radius of the bubble is expressed by the Rayleigh–Plesset equation

$$\rho(R\ddot{R} + \tfrac{3}{2}\dot{R}^2) = P_i - (P_\infty - P_A \cos \Omega t) - 2\sigma/R - 4\mu R/\dot{R} , \tag{4}$$

where σ is the surface tension, μ is the liquid viscosity, and P_i is the instantaneous pressure acting on the gas side of the bubble interface. In principle, this quantity must be determined by solving the pertinent conservation equations in the gas and in the liquid. For the case of linear oscillations the result of this calculation can be summarized by saying that thermal processes result in a pressure-volume relationship of the polytropic type

$$P_i = P_0(R_0/R)^{3\kappa} ,$$

where $P_0 = P_\infty + 2\sigma/R_0$ is the bubble internal pressure at equilibrium and κ is the polytropic exponent. The thermal processes contribute a dissipation mechanism[21–23] that can be represented by suitably modifying the value of the liquid viscosity. A further contribution to dissipation arises, because of acoustic radiation from the bubble, and this effect can also be accounted for by suitably modifying the value of μ.[23] Although it has been recently experimentally verified[24] that the description of these thermal processes via a polytropic exponent is adequate for small amplitude oscillations, an extension of these results to the case of large-amplitude, nonlinear oscillations which are of present concern has never been attempted. Accordingly, we are forced to use here the linear results for κ and the "effective" liquid viscosity, although Eq. (4) will be treated nonlinearly. In spite of this rather drastic approximation it will be seen that the theoretical results compare very favorably with experiment.

For radial pulsations of moderate amplitude one can obtain an approximate solution of Eq. (4) by writing $R = R_0[1 + x(t)]$ and performing a power series expansion in x. This procedure has been carried out in Ref. 4 to order of x^3 and we shall make use of those results in the following.

A. Linear approximation

The lowest-order approximation to the exact solution can be obtained by retaining only terms linear in x and its derivatives. In this way one readily finds

$$x = \frac{\xi \cos(\omega\tau + \delta)}{[(\omega^2 - \omega_0^2)^2 + 4b^2\omega^2]^{1/2}}.$$

In the above equation and in subsequent ones, the following terminology is used

$$\tau = (P_0/\rho)^{1/2}\, t/R_0, \quad w = 2\sigma/R_0P_0,$$
$$b = 2\mu/R_0(\rho P_0)^{1/2}, \quad \eta = P_A/P_\infty,$$
$$\xi = (1 - w)\eta, \quad \omega = R_0\Omega\,(\rho/P_0)^{1/2},$$
$$\omega_0^2 = 3\kappa - w, \quad \delta = \tan^{-1}[2b\omega/(\omega^2 - \omega_0^2)].$$

In particular ω_0 is the nondimensional resonance frequency of the bubble which, converted back to dimensional form, is given by the well-known expression

$$\Omega_0 = (1/R_0\rho^{1/2})[3\kappa P_\infty + (3\kappa - 1)(\sigma/R_0)]^{1/2}. \tag{5}$$

In the range of radius values of present concern the effect of the surface tension contribution is negligible and κ depends only weakly on R_0; thus this expression shows that the product $R_0\Omega_0$ is approximately a constant. If we define a resonance radius $R_{\rm res}$ by

$$\Omega = (1/R_{\rm res}\,\rho^{1/2})[3\kappa P_\infty + (3\kappa - 1)(\sigma/R_{\rm res})]^{1/2}, \tag{6}$$

we then have $\Omega/\Omega_0 \simeq R/R_{\rm res}$ which shows that, for fixed sound frequency Ω, we can vary the ratio Ω/Ω_0 by varying the radius of the bubble. In the figures, the data is displayed as a function of $R/R_{\rm res}$ because the experimental measurements were made in terms of variable radius rather than variable frequency.

To first order in x the time averages appearing in Eq. (3) are just $\langle (R/R_0)^3 \cos\Omega t\rangle \simeq 3\langle x\cos\Omega t\rangle$, $\langle (R/R_0)^3\rangle \simeq 1$ and we find

$$\mathscr{L}_e = \tfrac{3}{2}\xi B\cos\delta, \tag{7}$$

where

$$B = [(\omega^2 - \omega_0^2)^2 + 4b^2\omega^2]^{-1/2}.$$

For the case of small damping and for bubble radii sufficiently lower than the resonance radius, this result becomes

$$\mathscr{L}_e \simeq \left(\frac{3}{2}\right)\frac{1 - w}{3\kappa - w}\left(\frac{P_A}{P_\infty}\right). \tag{8}$$

For the range of bubble sizes investigated in this study w is very small ($w_{\rm res} \sim 10^{-2}$) and the polytropic exponent κ is only weakly dependent on R_0. Thus we find that the levitation number is only weakly dependent on the bubble radius if R_0 is much smaller than $R_{\rm res}$. It will be shown below that there is an important and measurable dependence of $\mathscr{L}_e$ on R_0 if the bubble is driven at an amplitude and frequency such that nonlinear effects are important.

B. Higher-order terms

If higher-order terms are retained in the solution of Eq. (4), harmonic and subharmonic resonances typical of nonlinear oscillations appear. The solution $x(\tau)$ in the harmonic and subharmonic regions, but not near the main resonance, is given by

$$\begin{aligned} x(\tau) = {} & A_n \cos\theta_n + \xi B\cos(\omega\tau + \delta) \\ & + (c_1 + \lambda_1 c_3 \cos 2\omega\tau)\xi^2 + (c_5 + c_2\cos 2\theta_n)A_n^2 \\ & + [c_4\cos(\omega\tau + \theta_n) + \lambda_2 c_0\cos(\omega\tau - \theta_n)]\xi A_n, \end{aligned} \tag{9}$$

where n is the order of the resonance, the c_i's are functions of ω given in the Appendix and $\theta_n = n\omega\tau + \phi_n$. The quantities λ_1, λ_2 are defined in the sections below and expressions for the amplitude A_n and phase ϕ_n of the resonance components are given in the Appendix.

Using the result expressed in Eq. (9) we can calculate explicitly the time averages entering in Eq. (3). Retaining only terms capable of giving nonzero contributions in the various harmonic resonance regions we find

$$\begin{aligned} \langle (R/R_0)^3\cos\omega\tau\rangle = {} & \tfrac{3}{2}B\xi\cos\delta + 3A_n\langle\cos\theta_n\cos\omega\tau\rangle \\ & + 3(c_2 + \tfrac{1}{2})A_n^2\cos 2\theta_n\cos\omega\tau \\ & + 3\xi A_n[\lambda_2 c_0\langle\cos\omega\tau\cos(\omega\tau - \theta_n)\rangle \\ & + B\langle\cos\omega\tau\cos(\omega\tau + \delta - \theta_n)\rangle]. \end{aligned} \tag{10}$$

Only terms consistent with the second-order accuracy of Eq. (9) have been retained in effecting the cube. Similarly we find

$$\langle (R/R_0)^3\rangle = 1 + 3(c_1 + \tfrac{1}{2}B^2)\xi^2 + 3(c_5 + \tfrac{1}{2})A_n^2.$$

This expression shows that in the quotient of averages in the right-hand side of Eq. (3), the denominator can be taken to be simply 1.0. Since an error of second order in the denominator is equivalent to an error of third order in the quotient, this approximation is consistent with the accuracy of Eqs. (9) and (10).

We now look specifically at the individual resonance regions.

1. $n = 2$ harmonic

For the $n = 2$ harmonic resonance ($\omega \simeq \omega_0/2$), $\lambda_1 = 0$ and $\lambda_2 = 1$. The amplitude A_2 and phase ϕ_2 are determined by Eqs. (A16) and (A17) of the Appendix. Setting $\theta_2 = 2\omega\tau + \phi_2$ and carrying out the time averages in Eq. (10) we obtain

$$\langle (R/R_0)^3\cos\omega\tau\rangle = \tfrac{3}{2}\xi\{B\cos\delta + A_2[c_0\cos\phi_2 + B\cos(\phi_2 - \delta)]\},$$

so that the theoretical levitation number takes the form

$$\mathscr{L}_e = \tfrac{3}{2}\xi\{B\cos\delta + A_2[c_0\cos\phi_2 + B\cos(\phi_2 - \delta)]\}. \tag{11}$$

For this $n = 2$ harmonic case, in addition to the previously obtained linear term ($\tfrac{3}{2}\xi B\cos\delta$), we find other terms that depend upon the amplitude and phase of the resonant component.

2. $n = 3$ harmonic

For the $n = 3$ harmonic resonance ($\omega \approx \omega_0/3$), $\lambda_1 = 1$, $\lambda_2 = 1$ and $\theta_3 = 3\omega\tau + \phi_3$. It is found that with this value of θ_3 all the averages in Eq. (10) vanish so that Eq. (3) reduces to the same form found for the linear approximation, Eq. (7).

3. Main resonance ($n = 1$)

For frequencies near the main resonance, $\omega \approx \omega_0$, and Eq. (9) is replaced by

$$x(\tau) = A_1 \cos(\omega\tau + \phi_1) + \tfrac{1}{2}[(4\omega^2 - \omega_0^2)^{-1} \cos(2\omega\tau - \phi_1) - \omega_0^{-2} \cos\phi_1]\xi A_1 + \tfrac{1}{2}[(\alpha_1 - \tfrac{3}{2}\omega^2)\omega_0^{-2} - (\alpha_1 + \tfrac{3}{2}\omega^2) \times (4\omega^2 - \omega_0^2)^{-1} \cos(2\omega\tau + 2\phi_1)]A_1^2 . \quad (12)$$

The amplitude A_1 and phase ϕ_1 are given by Eqs. (A19) and (A20) in the Appendix. Following the same procedure as before we readily find that for this case

$$\mathscr{L}_e = \tfrac{3}{2}A_1 \cos\phi_1 . \quad (13)$$

4. Polytropic exponent and damping

To evaluate some of the quantities entering into the above equations it is necessary to have expressions for the polytropic exponent and the damping constant. As stated previously, we shall make use of the results of the linear theory for these quantities. These results have been obtained by Eller[21] on the basis of a work by Devin[22] and by Prosperetti[23] using a somewhat different approach. In a recent paper,[24] it has been shown that under normal conditions, the two analytical results are essentially equal and that measurements of the polytropic exponent for a variety of gases and ranges of bubble sizes agree quite well with the analytical predictions. We give here, for completeness, expressions for the damping constants and the polytropic exponent.

The total damping constant b is the sum of the three principal contributions, i.e., viscous, radiation, and thermal. Thus

$$b = b_v + b_r + b_t ,$$

where

$$b_v = 2\mu/(\rho P_0)^{1/2} R_0 ,$$
$$b_r = \tfrac{1}{2}(\rho/P_0)^{1/2}(\Omega^2 R_0^2/c) ,$$
$$b_t = (\Omega_0^2 R_0/2\Omega)(\rho/P_0)^{1/2} d_t , \quad (14)$$

and

$$d_t = \frac{3(\gamma - 1)[X(\sinh X + \sin X) - 2(\cosh X - \cos X)]}{X^2(\cosh X - \cos X) + 3(\gamma - 1)X(\sinh X - \sin X)} ,$$

where c is the velocity of sound in the liquid, and γ is the ratio of specific heats of the gas contained within the bubble. Also $X = R_0(2\Omega/D_1)^{1/2}$, where D_1 is the thermal diffusivity of the gas defined as $D_1 = K_1/\rho_1 C_{p_1}$, K_1 is the thermal conductivity of the gas, ρ_1 is its density, and C_{p_1} its specific heat at constant pressure. The polytropic exponent κ is given by

$$\kappa = \gamma(1 + d_t^2)^{-1}\left[1 + \frac{3(\gamma - 1)}{X}\left(\frac{\sinh X - \sin X}{\cosh X - \cos X}\right)\right]^{-1} . \quad (15)$$

In order to obtain a final theoretical result for the levitation number as a function of the radius, we have combined the individual contributions given by Eqs. (7), (11), and (13) which are valid in their respective frequency regions. Some matching of the respective equations in the intermediate regions is required but this occurs rather naturally and presents no real problem.

III. RESULTS AND DISCUSSION

The main results of this study are given in Figs. 1 to 4 which compare the measured values of the levitation number $\mathscr{L}_e$ expressed in Eq. (3), with the theoretical predictions obtained from Eqs. (7), (11), and (13). The horizontal axis in these figures is the bubble radius R_0 normalized by the (theoretical) resonance radius R_{res} at the sound field frequency. For this present study, R_{res} was obtained from Eq. (6) with the polytropic exponent κ given by Eq. (15), and was approximately equal to 138 μm.

For the measurements and calculations used in these figures, one should assume that an air bubble is present in a glycerine–water mixture (38% by weight glycerine) and the values of the constants are as follows: $\rho = 1.09$ g/cm^3, $P_\infty = 1.01 \times 10^6$ dyn/cm^2, $\sigma = 70$ dyn/cm, $\mu = 0.03$ cm^{-1}·g·s^{-1}, $\Omega = 2\pi(22.2$ kHz), $D_1 = 0.20$ cm^2/s, $\gamma = 1.4$, $g = 9.8 \times 10^2$ cm/s^2, and $c = 1.61 \times 10^5$ cm/s. Shown in Fig. 1 are measurements of the levitation number of an air bubble in a glycerine–water mixture for an acoustic pressure amplitude of 0.095 bars as a function of the normalized bubble radius. It is seen that there is an oscillation in the magnitude of the levitation number as the bubble radius nears the normalized radius value of 0.5. Shown as a dotted line in this figure are the predictions of the linear theory. If one neglects the nonlinear terms, one should expect a normal resonance-type behavior as the bubble grows toward a normalized radius value of 1.0. Note that except for the oscillation near (R_0/R_{res}) = 0.5, there is a good fit to the linear theory over a wide

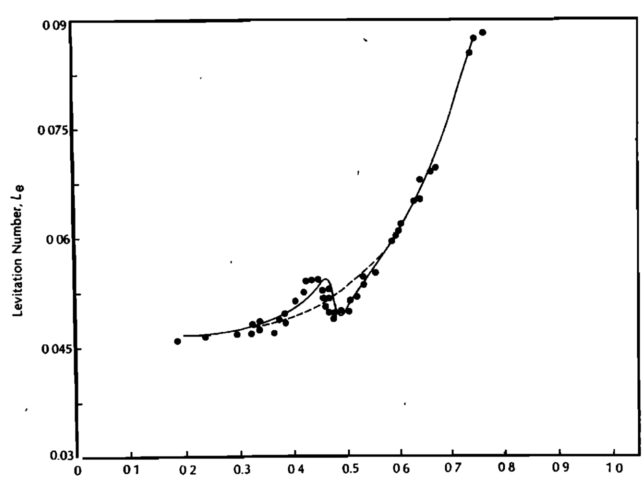

FIG. 1. Values of the levitation number for an air bubble in a glycerine–water mixture as a function of bubble size. The symbols are the experimental points and the dashed line is the prediction of the linear theory. The solid line represents a combination of the contributions from the individual resonance regions as predicted by a nonlinear theory. For this case, the acoustic pressure amplitude was 0.095 bars.

range of bubble radii. The solid curve on Fig. 1 represents the calculation of the nonlinear behavior of the bubble as represented by a combination of the contributions of Eqs. (7), (11), and (13). It is noted that the $n = 2$ harmonic contribution, Eq. (7), gives a nice fit to the data in this harmonic region. Equation (7) predicts that there will be no additional contribution to the linear term in the $n = 3$ harmonic region (although the bubble may be undergoing this harmonic pulsation, it should not show up experimentally). Finally, Eq. (13) also gives an excellent fit in the main resonance region for larger values of the bubble radius. The excellent fit at low radii in all the figures is partially artificial. In order to calibrate our levitation cell, we use a scheme proposed originally by Gould[25] in which we use the air bubbles themselves to calibrate the sound field within the cell. In short, this is done by introducing an air bubble into the levitation cell and measuring its radius and its position for a range of voltages obtained via the external hydrophone attached to the side of the levitation cell (see Fig. 1, Ref. 18). Using an expression for the acoustic pressure amplitude required to levitate a bubble of a particular radius at a particular position [which essentially involves the linear bubble oscillation expression, Eq. (7)], we can calibrate the levitation cell in terms of the voltages measured by the external hydrophone. We have checked this result to be accurate by removing the bubble and inserting at its former position a miniature, calibrated, probe hydrophone.

Figure 2 shows our results for an acoustic pressure amplitude of 0.155 bars. Note that $n = 2$ harmonic contribution has now become quite large and there is a rapid change in the magnitude of the levitation number near a normalized radius value of 0.5. This change is mostly due to a similarly rapid change in the phase angle associated with the $n = 2$ harmonic resonance, shown also on Fig. 2. It is seen that for a nearly constant value of A_2, $\cos\phi_2 \approx -1$ results in a much stronger Bjerknes force than for $\cos\phi_2 \approx +1$. Note again the excellent fit, especially of the magnitude of the harmonic contribution.

We present in Figs. 3 and 4 considerably larger values of the acoustic pressure amplitude, being 0.190 and 0.24 bars, respectively. For these relatively large values of the sound pressure it was not possible to track the bubble completely through the harmonic resonance. As the bubble pulsation amplitude became large, rectified diffusion would be so rapid that measurements of the bubble size near its harmonic maximum could not be made with great accuracy. Note, however, that the minimum values were obtained and show good agreement with the theory. It can be seen that the amplitude equation for the $n = 2$ harmonic region, Eq. (A16), is a cubic. If the acoustic pressure amplitude becomes sufficiently large, there are three real roots to this equation and pulsation amplitudes can change very rapidly.[4] The theoretical pressure amplitude required for the amplitude equation to be multiple-valued is approximately 0.28 bar, and since there is such good agreement between theory and experiment, we probably never reached this limit. However, for the highest pressure amplitude, $P_A = 0.24$ bar, we were sufficiently close to this limit to result in a very rapid change in phase angle as the bubble passed through this harmonic resonance.

The position of the experimental points on the graphs depends of course on the measured value of the equilibrium radius R_0. As was explained in Sec. I, this value was obtained by momentarily switching off the sound field and measuring the terminal rise velocity of the bubble. To obtain a value of the radius from the rise velocity it is necessary to utilize an expression for the drag force on the bubble. For the low Reynolds numbers of present concern we have used a modified form[26] of Stokes' law wherein the magnitude of the drag force on the bubble is expressed as

$$F_0 = 6\pi\mu R_0 u(1 + 0.20 R_e^{0.63} + 2.6\times10^{-4} R_e^{1.38}), \quad (16)$$

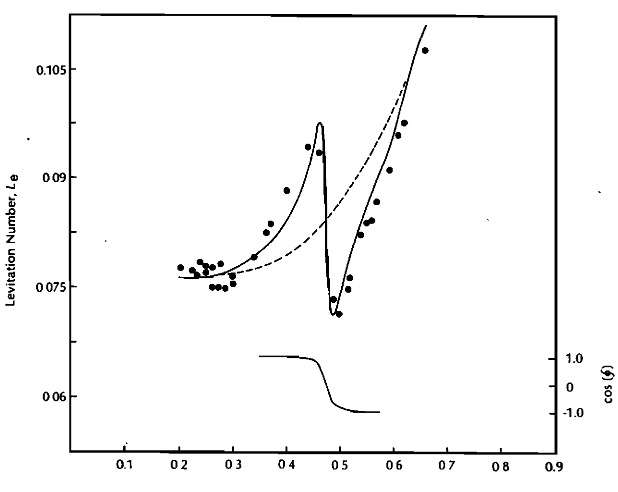

FIG. 2. Values of the levitation number for an air bubble in a glycerine–water mixture as a function of bubble size. The symbols are the experimental points and the dashed line is the prediction of the linear theory. The solid line represents a combination of the contributions from the individual resonance regions as predicted by a nonlinear theory. Shown also in this figure is the variation of the phase angle ϕ_2 as a function of radius. For this case, the acoustic pressure amplitude was 0.155 bars.

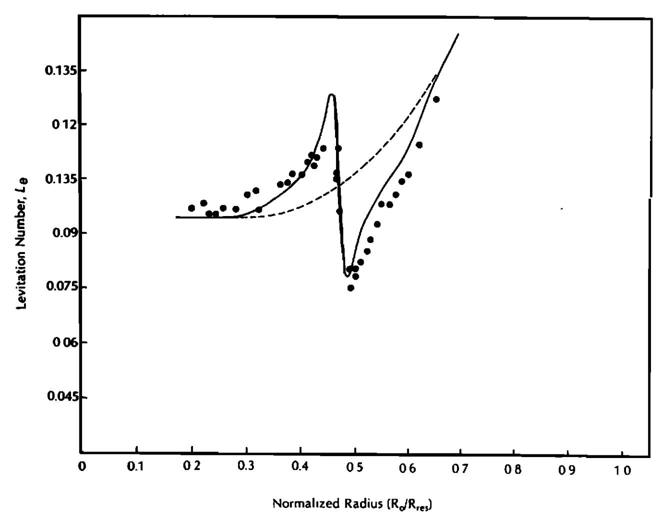

FIG. 3. Values of the levitation number for an air bubble in a glycerine–water mixture as a function of bubble size. The symbols are the experimental points and the dashed line is the prediction of the linear theory. The solid line represents a combination of the contributions from the individual resonance regions as predicted by a nonlinear theory. For this case, the acoustic pressure amplitude was 0.190 bars.

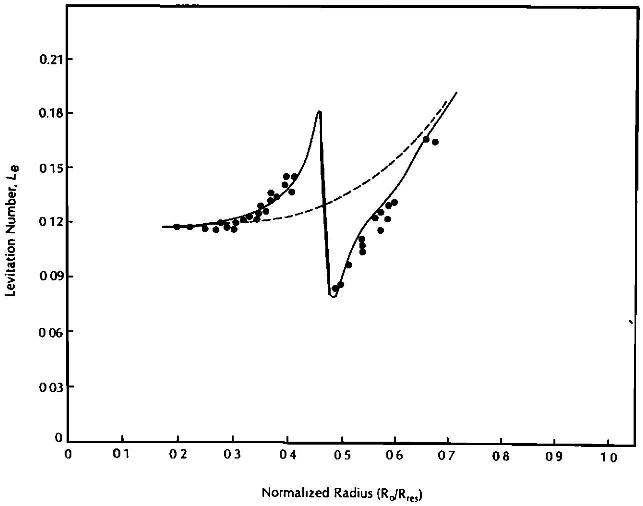

FIG. 4. Values of the levitation number for an air bubble in a glycerine–water mixture as a function of bubble size. The symbols are the experimental points and the dashed line is the prediction of the linear theory. The solid line represents a combination of the contributions from the individual resonance regions as predicted by a nonlinear theory. For this case, the acoustic pressure amplitude was 0.240 bars.

where u is the terminal rise velocity and R_e is the Reynolds number, given by $R_e = 2R_0 u\rho/\mu$. This expression has been shown to be applicable to the drag on solid spheres for a wide range of Reynolds numbers. Air bubbles in water are known to behave normally as solid spheres in terms of their drag characteristics, although theoretically they should experience a drag that is lower by a factor of 2/3 due to the anticipated slippage at the air–water interface.[28] The higher drag is usually attributed to surface contamination[29] and some recent experimental evidence[30] has demonstrated the gradual change from a slip to a no-slip regime as the bubble rises through the liquid. For this reason, an accurate drag prediction is not readily available. We have discovered that in approximately half of our data sets we could significantly improve the comparison between theory and experiment by shifting slightly the radii to lower values (this shift was at most 10%). If there was some partial slippage of the bubble interface, then the drag would be somewhat less than that for a solid sphere and the radii would need to be shifted to lower values. We believe that this slight shift in the radius values for some of the data sets is reasonable and confirms the applicability of our theory. Interestingly, this approach may provide a method for obtaining precise measurements of the radius for very small bubble sizes. Drag measurements on small bubbles are difficult to obtain because these bubbles will rapidly dissolve as they rise through the liquid. It is seen in these figures that the value of the bubble radius that gives rise to the minimum in the levitation number can be ascertained to within a few percent. Because the levitated bubble can be maintained at a fixed size by rectified diffusion and then permitted to rise a short distance while being viewed through a microscope, measurements of its drag characteristics could be easily obtained.

We have observed that under certain conditions, a bubble placed in our levitation cell will remain at a fixed radius for periods of time that approach several minutes. Since a bubble should either grow by rectified diffusion, or dissolve due to surface tension forces when it is below the rectified diffusion threshold, this behavior was considered by us to be anomalous. This very interesting effect can be explained, however, by inspection of the figures in this paper. Consider Fig. 3 and a bubble that has a radius intermediate in value between the levitation number minimum and maximum. If the bubble begins to dissolve, its pulsation amplitude will increase and thus it may exceed the threshold for growth by rectified diffusion and become larger. However, as it grows, its pulsation amplitude becomes smaller and it may then drop below the threshold and begin again to dissolve. If the conditions of gas saturation and driving amplitude are such as to permit this behavior to occur (as we believe we have observed) a bubble could be maintained indefinitely at a relatively constant radius. This effect may be useful in certain experiments.

IV. SUMMARY AND CONCLUSIONS

We have demonstrated that gas bubbles that are caused to pulsate in a liquid under the action of an acoustic pressure field can display nonlinear properties such as the presence of harmonic resonances in their oscillation. Measurements of the magnitude of the pulsation amplitude of the bubble near its $n = 2$ harmonic resonance are in excellent agreement with the predictions of theory. The amplitude of the pulsation near this resonance can vary greatly over a small radius band and be considerably larger than that predicted by a linear theory. Due to the possibility of large amplitude pulsations near these harmonic resonances, previous theories concerning the growth of bubbles by rectified diffusion[31] and of the shear stresses associated with pulsating bubbles may need to be modified to account for this nonlinear behavior.

We also wish to draw attention to the fact that the theoretical predictions involve many different aspects of bubble dynamics, of mechanical as well as thermal and acoustic in nature. The agreement between theory and experiment is therefore particularly significant because it implies that all these different aspects, both individually and in their mutual interplay, are correctly accounted for.

ACKNOWLEDGMENTS

We wish to gratefully acknowledge the financial support provided in part by the Office of Naval Research and the National Science Foundation in the United States and by Ministero Della Pubblica Istruzione in Italy. Travel funds provided by NATO permitting the close collaboration between the authors is also gratefully acknowledged. Finally, we wish to note the assistance of David Young in the acquisition of data and of Tim Farris and Gary Hansen with the computer programming.

APPENDIX

The form of the various functions of ω which appear in the text are given below. The auxiliary quantity D is defined as

$$D=(\omega_0^2-\omega^2)^{-1}$$

$$[\omega_0^2-(n-1)^2\omega^2]c_0(\omega)=D(\alpha_1-\tfrac{3}{2}n\omega^2)-\tfrac{1}{2}, \tag{A1}$$

$$\omega_0^2c_1(\omega)=\tfrac{1}{2}D\,[D(\alpha_1-\tfrac{3}{2}\omega^2)-1], \tag{A2}$$

$$(\omega_0^2-4n^2\omega^2)c_2(\omega)=\tfrac{1}{2}(\alpha_1+\tfrac{3}{2}n^2\omega^2), \tag{A3}$$

$$(\omega_0^2-4\omega^2)c_3(\omega)=\tfrac{1}{2}D\,[D(\alpha_1+\tfrac{3}{2}\omega^2)-1], \tag{A4}$$

$$[\omega_0^2-(n+1)^2\omega^2]c_4(\omega)=D(\alpha_1+\tfrac{3}{2}n\omega^2)-\tfrac{1}{2}, \tag{A5}$$

$$\omega_0^2c_5(\omega)=\tfrac{1}{2}(\alpha_1-\tfrac{3}{2}n^2\omega^2), \tag{A6}$$

$$\beta_2(\omega)=\tfrac{1}{2}D\,[D(\alpha_1+\tfrac{3}{2}\omega^2)-1], \tag{A7}$$

$$g_0(\omega)=\alpha_1(2c_5+c_2)+\tfrac{3}{2}n^2\omega^2(\tfrac{1}{4}-2c_2)-\tfrac{3}{4}\alpha_2, \tag{A8}$$

$$g_1(\omega)=-2\alpha_1c_1+c_4\{\tfrac{1}{2}-D\,[\alpha_1-\tfrac{3}{2}(n+1)\omega^2]\} + \tfrac{3}{2}(\alpha_2-\tfrac{1}{2}\omega^2)D^2-D, \tag{A9}$$

$$g_2(\omega)=c_0\{D\,[\alpha_1+\tfrac{3}{2}(n-1)\omega^2]-\tfrac{1}{2}\}, \tag{A10}$$

$$g_3(\omega)=c_6[D(\alpha_1+\tfrac{3}{2}\omega^2)-\tfrac{1}{2}]-2D^2\omega, \tag{A11}$$

$$g_4(\omega)=c_6(\alpha_1-\tfrac{3}{2}n\omega^2)+2(n-1)\omega D, \tag{A12}$$

$$d_1(\omega)=\tfrac{3}{4}\alpha_2-\alpha_1[\omega_0^{-2}(\alpha_1-\tfrac{3}{2}\omega^2) + \tfrac{1}{2}(\alpha_1+\tfrac{3}{2}\omega^2)(\omega_0^2-4\omega^2)^{-1}] - \tfrac{3}{2}\omega^2[\tfrac{1}{4}-(\alpha_1+\tfrac{3}{2}\omega^2)(\omega_0^2-4\omega^2)^{-1}], \tag{A13}$$

$$d_2(\omega)=\tfrac{3}{4}(\alpha_1-\tfrac{3}{2}\omega^2)(\omega_0^2-4\omega^2)^{-1}+\tfrac{3}{2}\omega_0^{-2}(\alpha_1-\tfrac{1}{2}\omega^2)-\tfrac{3}{4}, \tag{A14}$$

$$d_3(\omega)=\tfrac{1}{4}(\alpha_1-\tfrac{15}{2}\omega^2)(\omega_0^2-4\omega^2)^{-1}+\tfrac{1}{2}\omega_0^{-2}(\alpha_1-\tfrac{3}{2}\omega^2)-\tfrac{1}{4}. \tag{A15}$$

For the $n=2$ harmonic resonance, the amplitude A_2 and phase ϕ_2 are determined from the following equations:

$$g_0^2A_2^6+2g_0Q_2A_2^4+(Q_2^2+16b^2\omega^2)A_2^2-\xi^2\beta_2^2=0, \tag{A16}$$

$$\sin\phi_2=\frac{bA_2g_3(Q_2+g_0A_2^2)-4\omega\beta_2}{\xi^2\beta_2^2}, \tag{A17}$$

where

$$Q_2=4\omega^2-\omega_0^2-\xi^2(g_1-g_2). \tag{A18}$$

For the main resonance, the amplitude A_1 and phase ϕ_1 are solutions of the following equations:

$$2\omega bA_1+\xi(1-d_3A_1^2)\sin\phi_1+\tfrac{1}{4}\xi^2A_1\omega_0^{-2}\sin 2\phi_1=0. \tag{A19}$$

$$A_1[\omega^2-\omega_0^2+\tfrac{1}{2}\xi^2(2\omega^2-\omega_0^2)\omega_0^{-2}(4\omega^2-\omega_0^2)^{-1}] - d_1A_1^3+\xi(1-d_2A_1^2)\cos\phi_1 + \tfrac{1}{4}\xi^2A_1\omega_0^{-2}\cos 2\phi_1=0. \tag{A20}$$

[1]W. Lauterborn, J. Acoust. Soc. Am. **59**, 283–293 (1976).
[2]A. I. Eller and H. G. Flynn, J. Acoust. Soc. Am. **46**, 722–727 (1969).
[3]M. H. Safar, J. Phys. D **3**, 635–636 (1970).
[4]A. Prosperetti, J. Acoust. Soc. Am. **56**, 878–885 (1974).
[5]A. Prosperetti, J. Acoust. Soc. Am. **57**, 810–821 (1975).
[6]R. Esche, Acustica **2**, 208–218 (1952).
[7]P. de Santis, D. Sette, and F. Wanderlingh, J. Acoust. Soc. Am. **42**, 514–516 (1967).
[8]P. W. Vaughn, J. Sound Vib. **7**, 236–246 (1968).
[9]E. A. Neppiras, J. Sound Vib. **10**, 176–186 (1969).
[10]E. A. Neppiras, Physics Repts. **61**, 160–185 (1980).
[11]E. A. Neppiras, J. Acoust. Soc. Am. **46**, 587–600 (1968).
[12]W. T. Coakley, J. Acoust. Soc. Am. **49**, 792–798 (1971).
[13]J. W. Morris and W. T. Coakley, J. Sound Vib. **6**, 113–118 (1980).
[14]F. G. Sommer and D. Pounds, Med. Phys. **9**, 1–3 (1982).
[15]D. L. Storm, "Frequency spectrum of Finite Amplitude Radiation from the Nonlinear Pulsation of a Gas Bubble," Ph.D. thesis, University of Vermont (1975).
[16]D. L. Miller, Ultrasonics **19**, 217–224 (1981).
[17]A. I. Eller, J. Acoust. Soc. Am. **43**, 170–171 (1968).
[18]L. A. Crum, J. Acoust. Soc. Am. **68**, 203–211 (1980).
[19]R. E. Apfel, New Scientist **84**, 857–859 (1979).
[20]L. A. Crum, J. Acoust. Soc. Am. **57**, 1363–1370 (1975).
[21]A. I. Eller, J. Acoust. Soc. Am. **47**, 1469–1470 (1970).
[22]C. Devin, J. Acoust. Soc. Am. **31**, 1654–1667 (1959).
[23]A. Prosperetti, J. Acoust. Soc. Am. **61**, 17–27 (1977).
[24]L. A. Crum, "The Polytropic Exponent of Gas Contained within Air Bubbles Pulsating in a Liquid," J. Acoust. Soc. Am. **73**, 116–120 (1983).
[25]R. K. Gould, J. Acoust. Soc. Am. **43**, 1185–1186 (1968).
[26]L. A. Crum and A. I. Eller, "The Motion of Air Bubbles in a Stationary Sound Field," Tech. Memo. No. 61, Acoustics Research Laboratory, Harvard University (1969).
[27]I. Langmuir, "Mathematical Investigation of Water Droplet Trajectories," in *The Collected Works of Irving Langmuir*, Vol. 10, *Atmospheric Phenomena* (Pergamon, New York, 1961), pp. 348–393.
[28]W. L. Haberman and R. K. Morton, "An Experimental Investigation of the Drag and Shape of Air Bubbles Rising in Various Liquids," David Taylor Model Basin Rep. No. 802 (1953).
[29]R. Clift, J. R. Grace, and M. E. Weber, *Bubbles, Drops and Particles* (Academic, New York, 1978).
[30]A. Detiviler and D. C. Blanchard, Chem. Eng. Sci. **33**, 9–13 (1978).
[31]L. A. Crum and G. M. Hansen, "Generalized Equations for Rectified Diffusion," J. Acoust. Soc. Am. **72**, 1586–1592 (1982).